

From multiply twinned to fcc nanoparticles via irradiation-induced transient amorphization

This content has been downloaded from IOPscience. Please scroll down to see the full text.

2009 EPL 85 26001

(<http://iopscience.iop.org/0295-5075/85/2/26001>)

View [the table of contents for this issue](#), or go to the [journal homepage](#) for more

Download details:

IP Address: 128.214.177.188

This content was downloaded on 01/04/2014 at 09:02

Please note that [terms and conditions apply](#).

From multiply twinned to fcc nanoparticles via irradiation-induced transient amorphization

T. T. JÄRVI^{1(a)}, D. POHL², K. ALBE³, B. RELINGHAUS², L. SCHULTZ², J. FASSBENDER⁴, A. KURONEN¹ and K. NORDLUND¹

¹ Department of Physics, University of Helsinki - P.O. Box 43, FI-00014 Helsinki, Finland, EU

² IFW Dresden, Institute for Metallic Materials - P.O. Box 270116, D-01171 Dresden, Germany, EU

³ Institut für Materialwissenschaft, Technische Universität Darmstadt - Petersenstr. 23, D-64287 Darmstadt, Germany, EU

⁴ Institute of Ion Beam Physics and Materials Research, Forschungszentrum Rossendorf - P.O. Box 510119, D-01314 Dresden, Germany, EU

received 14 August 2008; accepted in final form 13 December 2008

published online 22 January 2009

PACS 64.70.Nd – Structural transitions in nanoscale materials

PACS 61.43.Dg – Amorphous semiconductors, metals, and alloys

PACS 61.80.-x – Physical radiation effects, radiation damage

Abstract – We present experimental evidence for structural transformation of multiply twinned CuAu nanoparticles to single-crystalline morphology by 0.5 keV helium irradiation. This finding is unexpected as the stability of twin boundaries should not be affected by ion-beam-induced Frenkel pairs. Molecular-dynamics simulations reveal, however, a new transformation mechanism based on transient amorphization of the particle. By comparing with irradiation simulations of elemental nanoparticles, as well as alloyed bulk samples and surface cascades, we show that this transformation route is only present in alloyed particles. Moreover, the observed amorphization is more efficient for twinned than single-crystalline particles. This, together with the fast recrystallization kinetics in CuAu, explains the experimentally observed untwinning process.

Copyright © EPLA, 2009

Introduction. – The structure of nanoparticles generally has a strong influence on their physical properties. In particular, the magnetic properties of binary transition metal particles depend strongly on their structure [1]. Ion irradiation of supported particles is a means to induce structural phase transformations and thus allows for some control over the particle properties. For example, the L1₀-order in FePt particles is enhanced by He-irradiation due to the production of athermal vacancies [2]. FePt particles also undergo structural transformation from multiply twinned icosahedral (I) to single-crystalline (SC) fcc structures upon 5 keV He-irradiation [3]. The mechanism of this transformation, however, is unclear as one would not expect irradiation-induced Frenkel pairs to remove twin boundaries. Recently, we showed [4] that twinned elemental Pt particles with a high thermodynamic driving force for untwinning remain unaltered under irradiation, thus leaving the transformation mechanism in alloyed particles an open question.

In the present letter, we elucidate the response of CuAu nanoparticles to light ion irradiation and propose a mechanism for the irradiation-induced untwinning. Similar to FePt, bulk CuAu exhibits L1₀ ordering in its bulk equilibrium state, providing another system where the effect of ion irradiation can be studied both with experiments and molecular dynamics simulations.

Methods. –

Experimental. CuAu nanoparticles with mean diameter of about 5 nm and a narrow-size distribution were prepared through inert gas condensation at a pressure of $p_{\text{Ar}} = 1.5$ mbar. After nucleation and growth within an aggregation volume, they were ejected into high vacuum via differential pumping and deposited onto carbon-coated nickel grids [5]. The particles were well separated on the surface, with an average interparticle distance of 10 nm. Structural characterization was carried out with high-resolution transmission electron microscopy (HRTEM) using aberration-corrected FEI Titan³ 80-300 and Philips Tecnai F30 microscopes (both operated at 300 keV and

^(a)E-mail: tommi.t.jarvi@helsinki.fi

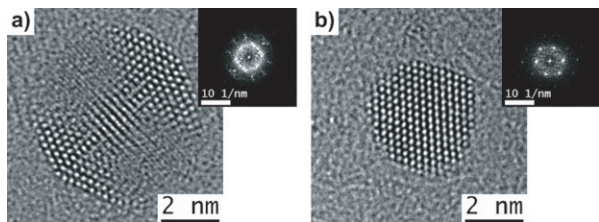


Fig. 1: Typical CuAu-particle morphologies before and after He^+ irradiation. a) Before: Icosahedron along its twofold symmetry axis. b) Single-crystal particle found after irradiation. (The insets show the Fourier transform of the original image.)

equipped with field emission guns). The composition of the particles was analysed using energy dispersive X-ray spectrometry (EDXS). As the beam size size is much larger than the nanoparticles, we measured the average nanoparticle composition over an area of about $(100 \text{ nm})^2$.

The as-prepared particles were irradiated with 0.5 keV helium ions at a relatively high fluence of $3 \cdot 10^{17}$ ions/cm² at room temperature. The irradiation was carried out under high-vacuum conditions using the low-energy ion implanter DANFYSIK 1050 with an ion current density of $2 \mu\text{A}/\text{cm}^2$.

Theoretical. To investigate the energetics of the particles and the kinetics of the irradiation process, we applied molecular-dynamics simulations. Interatomic interactions were described by the embedded-atom-method [6] (EAM) potentials of Foiles *et al.* [7]. (Other potentials will be discussed below). At short distances these were smoothly joined to the universal repulsive Ziegler-Biersack-Littmark potentials [8] that were also used to describe the ion-metal-interactions. Inelastic energy losses due to electronic stopping were included for atoms with kinetic energy higher than 5 eV [8].

Results. – Thorough statistical analysis by HRTEM revealed that the as-prepared particles were predominantly multiply twinned particles (MTPs) of icosahedral structure. In fig. 1a), such a particle is shown along its twofold symmetry axis with the power spectra, obtained by fast Fourier transformation (FFT) of the original image. The as-deposited particles were found to be chemically disordered, the composition being $\text{Cu}_{50}\text{Au}_{50}$ within an accuracy of ± 3 at.%.

After irradiation the structural analysis indicated that the as-prepared icosahedral MTPs had transformed into other morphologies like single-crystalline, singly twinned, and decahedral particles. In particular, a dramatic untwinning was observed, with 64% of the particles being single crystalline after irradiation. The percentages of different morphologies before and after irradiation are given in table 1.

As the crystal structure of every individual particle is visible in the HRTEM, ordered particles are identified by a superstructure in the diffractogram. No promotion of the

Table 1: Structural characterization of the CuAu nanoparticles before and after 0.5 keV helium irradiation. All values are percentages obtained by counting ~ 150 particles.

	Single crystalline	Icosahedral	Other
before	2	58	40
after	64	3	33

L_{10} ordering was observed upon irradiation, demonstrating that the percentage of ordered particles must be at least below 1%.

For fluences as high as used here, sputtering becomes important especially for nanoparticles [9], the mean particle diameter decreasing from 5.6 to 3.3 nm. Also, somewhat surprisingly, the particle composition did not change within the experimental uncertainty given above, even though some preferential sputtering effects could be expected. A SRIM [10] calculation indicates that in random CuAu, the sputtering yields of the components under 0.5 keV He irradiation are 0.084 for Cu and 0.059 for Au atoms (both ± 0.002). However, one should note that the surface is expected to be enriched by Au because of its lower surface energy, the same being observed for Pt in FePt [11]. Surface-enrichment will thus compensate for preferential sputtering. Also, the surface-enrichment will protect the particles from oxidation.

The above results are in line with previous experiments on FePt particle irradiation [3], where also lower fluence effects were discussed. We have also made additional experiments on both FePt and CuAu irradiation at different energies, showing similar results. This work will be discussed in detail elsewhere [12].

The fact that elemental metal nanoparticles do not seem to untwin under irradiation [4] suggests that the mechanism is related to the alloyed nature of the system. In order to elucidate the difference between alloyed and elemental particles, we applied molecular-dynamics simulations to investigate the energetics of the particles and the kinetics of the irradiation process.

To study the effect of irradiation on CuAu nanoparticles, we simulated consecutive 3 keV helium impacts on a free, chemically disordered, 3871 atom icosahedral particle. (0.5 keV and 3 keV ions produce qualitatively similar cascades. Experiments at other energies than 0.5 keV will be reported elsewhere [12].) The same procedure was used before for He irradiation of twinned Pt particles and is described in detail in ref. [4].

Surprisingly, and in contrast to the results for elemental Pt and Au [4,9], the simulations show that amorphization takes place for CuAu nanoparticles under irradiation. The average number of amorphized atoms per incoming ion was ~ 4 (see footnote ¹).

¹Amorphous atoms were detected using the algorithm, based on bond correlation using spherical harmonics, described in ref. [13]. With this analysis, the atoms could be separated to amorphous (liquid-like) and crystalline (fcc, grain boundary, etc., with correlated bonds) ones almost perfectly, giving a working definition of an amorphous atom.

In order to elucidate whether the finding of amorphization in twinned particles is a result of the alloyed nature, the internal structure, or the finite size, we carried out additional simulations of consecutive 300 eV cascades in defect free bulk CuAu samples as well as cascades close to a surface and twin boundary. As grain boundaries may enhance amorphization [14,15], the (111)-orientation was chosen for the bulk surface system and a stacking, where every fourth atomic layer was a twin boundary, was created. In all systems, Cu and Au were chemically disordered, as such was the case for the experimentally irradiated particles.

A cascade was initiated by giving a random atom the above recoil energy in a random direction and letting the system thermalize for 25 ps from the start of the cascade. In the case of nanoparticles, the particle was placed in vacuum and quenched to 0 K before a new cascade was started. In bulk, uniform irradiation was achieved by translating the system randomly around the periodic boundaries before each cascade. The recoil was then initiated in the center of the cell (in the surface case, this was done only in directions perpendicular to the surface) and temperature control was applied on the (non-open) cell boundaries. The amorphization as a function of the number of cascades was determined by averaging over 10 series of cascades.

In the bulk cases, both with and without the surface and stacking faults, no amorphization occurred. It is thus clear that the alloyed nature of the system is not sufficient to cause amorphization. This is in accord with previous results as, although there are to our knowledge no prior experimental irradiation studies of CuAu, irradiation of bulk Cu₃Au and FePt have been reported [16–20], but with no signs of amorphization. Few models are available to judge the amorphization susceptibility of a specific alloy under irradiation, one such model being the segregation charge transfer model [21]. Also according to this, neither FePt nor CuAu should amorphize under irradiation in bulk.

Cascades in the ~ 4 nm nanoparticle, on the other hand, caused amorphization with a steady rate, as shown in fig. 2. The amorphization tended to initiate at the particle surface, although also the inner parts were amorphized before the whole surface lost its crystallinity. The easier amorphizability of the particle compared to the bulk systems is mainly due to two effects. First, contrary to what happens in bulk, the interstitial component of a Frenkel pair produced by irradiation is able to escape, greatly diminishing the ballistic recombination probability of Frenkel pairs and thus allowing for an increased vacancy concentration as compared to the bulk case. Second, the vacancy-induced strain fields destabilize the lattice structure, an effect which is even more pronounced in an alloy with different atomic radii. Due to the close vicinity of the particle surface, the elastic driving force for restoring the lattice is much smaller than in the bulk case and the particle stays amorphous.

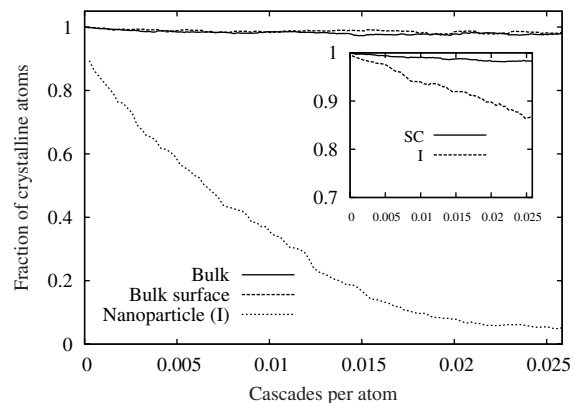


Fig. 2: Fraction of crystalline atoms as a function of the number of 300 eV cascades per atom in the icosahedral CuAu nanoparticle and bulk. The inset shows the cases of single-crystalline (SC) and icosahedral (I) FePt nanoparticles. (The particle sizes are 3871 (I) and 3739 (SC) atoms.)

The conclusion from the above discussion is that we observe an obvious difference between the response of nanoparticles and bulk matter to He irradiation. Further, neither the alloyed nature of the system nor the nanocrystallinity by itself produces amorphization under irradiation, both being needed to sufficiently destabilize the crystalline phase. This leads to a transformation route that has not been considered for binary metallic alloys. In the following, we establish the connection between amorphization and the experimentally observed untwinning. We discuss first the role of particle morphology in amorphization and then the kinetics of recrystallization by which the crystalline phase is restored.

To study the role of the particles' morphology in the amorphization, the cascade simulation described above was repeated for a single-crystalline CuAu particle of similar size, but essentially the same rate of amorphization was found as for the icosahedral particle. This is because the Foiles potential, typically for EAM, underestimates the stacking fault energies, making the I and SC phases similar in energy.

Thus, in order to reveal the role of particle structure on amorphization, as well as to verify the amorphization for another alloy, the particle cascade simulations were repeated for FePt by means of an angular-dependent bond-order potential (BOP) [22]. In FePt, the energy difference between icosahedral and single-crystalline particles is very high and is accurately described by the BOP, the twin boundary energy being $\gamma_{TB} = 166 \frac{\text{mJ}}{\text{m}^2}$. (see ref. [23] for a detailed discussion). The resulting progress of amorphization is shown in the inset of fig. 2. Now, the rate of amorphization for the icosahedral phase is over a factor of two higher than that for the single-crystalline one, demonstrating that the presence of twin planes affects the material's behavior under ion irradiation. This result is in accordance with previous studies, where amorphization has been found to occur preferentially near grain boundaries [14,15].

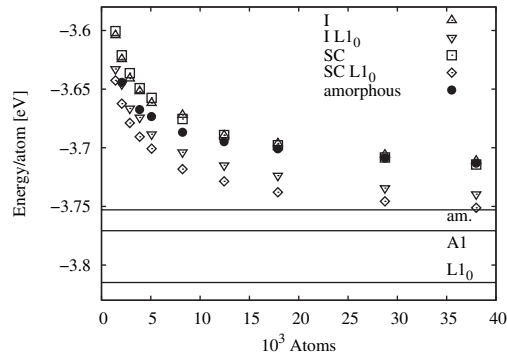


Fig. 3: Energies of chemically ordered ($L1_0$) and disordered icosahedral (I), single-crystalline (SC), and amorphous CuAu particles with the Foiles potential. Energies of bulk phases are shown as horizontal lines.

The next question that has to be addressed is the connection between amorphization and the experimentally observed disappearing of grain boundaries, as no amorphous structures were observed in the experiments. The critical factors are the stability of the ion-induced amorphous structure and the recrystallization rate. In order to estimate thermodynamic driving forces, the energies of amorphous², icosahedral and single-crystalline CuAu particles were calculated for ordered and disordered configurations (see fig. 3). The amorphous particles are thermodynamically not stable but relatively low in energy. The recrystallization kinetics are thus crucial for the occurrence of the amorphous phase.

We estimated the possible range of values for the recrystallization activation energy from a simple kinetic consideration. An effective recrystallization rate can be written as

$$dN_{\text{am}}/dt = -N_{\text{am}}\Gamma_0 e^{-E/kT}, \quad (1)$$

N_{am} being the number of amorphous atoms. As parameters, we used a particle radius of 2.2 nm and the experimental irradiation parameters above, with a prefactor of $\Gamma_0 = \frac{1}{\text{ps}}$. A damage production of 4 atoms per He, obtained above from the simulation taking the impacting He ions into account explicitly, was used.

Two limiting cases can be used to set bounds on the activation energy. Considering the amount of damage produced by a single ion, after the time it takes on average for the next ion to impact, gives (at 300 K), a limit of ~ 0.7 eV for the activation energy. For values lower than this, there is some healing before the next ion impact. On the other hand, consider a 3000 atom particle, assumed to be completely amorphized by irradiation. Such a particle

²Amorphous particles were prepared by cooling a molten particle with a rate of 1 K/ps. In the process, the particle surface was enriched with gold but the inner part was left homogeneous. The energy difference between a particle obtained in this manner and one where the surface was made copper-enriched by reversing the atomic species was notable, *e.g.*, ~ 40 meV/atom for the 3871 atom particle, illustrating the range of energies of different amorphous configurations.

should crystallize in, say, 24 h in order not to be observed in the present experimental setup. This restriction gives an upper limit of ~ 1 eV to the activation energy, a value consistent with previous results [24], where the same limiting value was found to be required for amorphization of bulk intermetallics. For values between the two limits, the particle would be amorphized completely by the irradiation and subsequently recrystallized.

The recrystallization barrier from the amorphous to the crystalline phase for the Foiles potential was determined³ to be 60 meV below and 300 meV above the glass transition temperature (~ 400 K), displaying behavior similar to diffusion in amorphous alloys [25].

Such a low barrier indicates that amorphized CuAu would not be observed in experiments without other factors, such as an amorphous matrix, hindering recrystallization. The experimental scenario is clearly the domain where the particle only amorphizes partially. The rate of damage production, obtained above from the simulation taking the ions into account explicitly, would predict full amorphization with a dose of $4 \cdot 10^{15} \frac{1}{\text{cm}^2}$ in a scenario without healing, a dose two orders of magnitude lower than the one used in the experiment. The high recrystallization rate obtained from the Foiles potential, and the fact that amorphous (bulk) CuAu and FePt have not been observed upon irradiation, shows that instead of amorphizing completely, the particles experience some healing during irradiation. This is in agreement with the large dose required to induce the structural transformation.

The grain boundaries thus disappear due to migration caused by recrystallizing amorphous pockets. It has been shown [26] that collision cascades cause bending/migration of high-angle grain boundaries. The same effect is observed in the present case, for twin boundaries in the presence of recrystallizing amorphous pockets. To demonstrate this in a model system, we created an amorphous pocket on top of a planar twin boundary in FePt. (FePt was chosen since the BOP reproduces its twin boundary energy, $\gamma_{TB} = 166 \frac{\text{mJ}}{\text{m}^2}$.) The pocket was created with a vacancy concentration of 5% mimicking that corresponding to an irradiated alloy. Subsequent annealing of the pocket at a high temperature (1400 K) for 0.5 ns resulted in the configuration shown in fig. 4, where the atoms have been colored according to their structure, as determined using common neighbour analysis [27]. The recrystallization has led to a part of the twin boundary migrating by one atomic layer.

Thus, successive recrystallization of amorphous pockets created by the irradiation will allow for the bending/migration of the twin boundaries. This, together with the thermodynamic driving force to untwin and the preference to amorphize near grain boundaries, leads to

³The barrier was determined by simulating a half-amorphous, half-crystalline cell at several temperatures ranging from 100 K to 700 K. Recrystallization rates were obtained by following the number of crystalline atoms as a function of time for roughly 1 ns. An Arrhenius equation was fitted to the rates thus obtained.

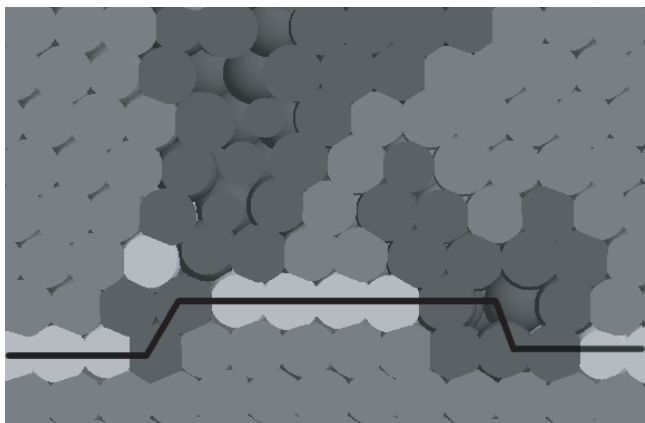


Fig. 4: Recrystallized amorphous pocket in FePt, showing a bent twin boundary (line) as well as clustered vacancies. The atoms have been shaded according to structure: twin boundary (lightest), fcc, and other (darkest).

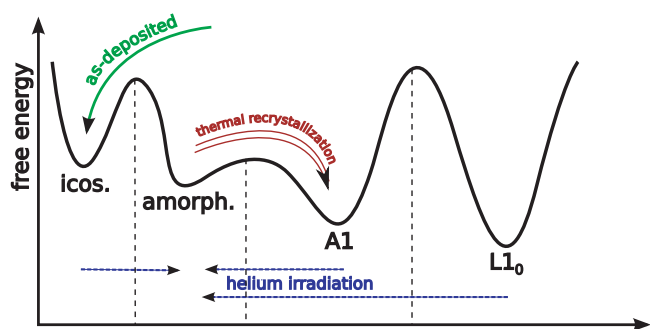


Fig. 5: Schematic free-energy plot illustrating the proposed mechanism. Thermal recrystallization of amorphous pockets created by irradiation allows the particles to reach the single-crystalline A1 phase.

the annihilation of the twins. The main elements of the process are illustrated in fig. 5.

Discussion. – To our knowledge, this is the first time amorphization of nanoparticles has been reported for alloys that do not amorphize in bulk. It should be noted, however, that previous studies have provided hints of a similar effect in embedded metal clusters [28], although for embedded particles, the effect of mixing with the matrix cannot easily be excluded. Moreover, evidence for reduced resistance to amorphization has turned up for nanocrystals and embedded nanoalloys [15,29,30] (that do amorphize in bulk) and it is well known that bimetallic systems have a lower amorphization threshold than elemental ones [31]. Also, although we observe the same transformation for two alloys simulated by different potential types, it remains to be shown to what extent this result can be generalized for other binary alloys.

As $L1_0$ ordering was observed in neither the as-prepared nor the irradiated particles, we have limited our discussion to disordered systems. Ordering should be expected, however, to have some effect on amorphization. Indeed,

in cascade simulations of the kind described above (but not shown), ordered particles were found to amorphize somewhat slower than disordered ones.

Conclusions. – Experimental evidence and atomistic simulations indicate that untwinning upon irradiation occurs via transient amorphization. This happens for bimetallic alloys that do not amorphize in bulk. We show that the resistance to amorphization of alloy nanoparticles is drastically reduced compared to bulk, even when the particles are not embedded in an amorphous matrix. This effect is the decisive factor in the untwinning transformation, along with a preference to amorphize near grain boundaries.

Further investigation of the transformation is, however, required. Specifically, a crucial test would be to conduct irradiation experiments on elemental particles to confirm the absence of structural transformation [4]. Another intriguing possibility is preventing the recrystallization, using for example low temperature, and observing the amorphous nanoparticles.

A part of this work was performed within the Finnish Centre of Excellence in Computational Molecular Science (CMS). We also gratefully acknowledge support within an exchange program from the Academy of Finland and the German Foreign Exchange Service (DAAD), as well as the grants of computer time from CSC, the Finnish IT centre for science.

REFERENCES

- [1] GRUNER M. E., ROLLMANN G., ENTEL P. and FARLE M., *Phys. Rev. Lett.*, **100** (2008) 087203.
- [2] WIEDWALD U., KLIMMER A., KERN B., HAN L., BOYEN H.-G., ZIEMANN P. and FAUTH K., *Appl. Phys. Lett.*, **90** (2007) 062508.
- [3] DMITRIEVA O., RELINGHAUS B., KÄSTNER J., LIEDKE M. O. and FASSBENDER J., *J. Appl. Phys.*, **97** (2005) 10N112.
- [4] JÄRVI T. T., KURONEN A., NORDLUND K. and ALBE K., *J. Appl. Phys.*, **102** (2007) 124304.
- [5] SCHÄFFEL F., KRAMBERGER C., RÜMMELI M. H., KALTOFEN R., GRIMM D., GRÜNEIS A., MOHN E., GEMMING T., PICHLER T., BÜCHNER B., RELINGHAUS B. and SCHULTZ L., *Phys. Status Solidi A*, **204** (2007) 1786.
- [6] DAW M. S. and BASKES M. I., *Phys. Rev. B*, **29** (1984) 6443.
- [7] FOILES S. M., BASKES M. I. and DAW M. S., *Phys. Rev. B*, **33** (1986) 7983.
- [8] ZIEGLER J. F., BIERSACK J. P. and LITTMARK U., *The Stopping and Range of Ions in Matter* (Pergamon, New York) 1985.
- [9] JÄRVI T. T., PAKARINEN J. A., KURONEN A. and NORDLUND K., *EPL*, **82** (2008) 26002.

- [10] ZIEGLER J. F., SRIM-2008 software package, available online at www.srim.org.
- [11] WANG R. M., DMITRIEVA O., FARLE M., DUMPICH G., YE H. Q., POPPA H., KILAAS R. and KISIELOWSKI C., *Phys. Rev. Lett.*, **100** (2008) 017205.
- [12] POHL D., MOHN E., RELINGHAUS B., FASSBENDER J. and SCHULTZ L., unpublished.
- [13] MENDEZ-VILLUENDAS E. and BOWLES R. K., *Phys. Rev. Lett.*, **98** (2007) 185503.
- [14] GOO E., MURTHY A. and HETHERINGTON C. J. D., *Scr. Metall. Mater.*, **29** (1993) 553.
- [15] OVID'KO I. A. and SHEINERMAN A. G., *Appl. Phys. A*, **81** (2005) 1083.
- [16] JENKINS M. L. and ENGLISH C. A., *J. Nucl. Mater.*, **108-109** (1982) 46.
- [17] IVCHENKO V. A. and SYUTKIN N. N., *Appl. Surf. Sci.*, **87-88** (1995) 257.
- [18] BATTAGLIN G., CARNERA A., KULKARNI V. N., RUSSO S., MAZZOLDI P. and CELOTTI G., *Thin Solid Films*, **131** (1985) 69.
- [19] LAI C.-H., YANG C.-H. and CHIANG C. C., *Appl. Phys. Lett.*, **83** (2003) 4550.
- [20] MORGAN N. W., BIRTCHER R. C. and THOMPSON G. B., *J. Appl. Phys.*, **100** (2006) 124904.
- [21] OSSI P. M. and PASTORELLI R., *Nanostruct. Mater.*, **11** (1999) 739.
- [22] MÜLLER M., ERHART P. and ALBE K., *Phys. Rev. B*, **76** (2007) 155412.
- [23] MÜLLER M. and ALBE K., *Acta Mater.*, **55** (2007) 6617.
- [24] SIMONEN E. P., *Nucl. Instrum. Methods Phys. Res. B*, **16** (1986) 198.
- [25] FAUPEL F., FRANK W., MACHT M.-P., MEHRER H., NAUNDORF V., RÄTZKE K., SCHOBER H. R., SHARMA S. K. and TEICHLER H., *Rev. Mod. Phys.*, **75** (2003) 237.
- [26] VÖGELI W., Master's Thesis, TU Darmstadt, Germany (2004).
- [27] HONEYCUTT J. D. and ANDERSEN H. C., *J. Phys. Chem.*, **91** (1987) 4950.
- [28] JOHANNESSEN B., KLUTH P., LIEWELLYN D. J., FORAN G. J., COOKSON D. J. and RIDGWAY M. C., *Appl. Phys. Lett.*, **90** (2007) 073119.
- [29] MELDRUM A., BOATNER L. A. and EWING R. C., *Phys. Rev. Lett.*, **88** (2002) 025503.
- [30] DJURABEKOVA F., BACKMAN M. and NORDLUND K., *Nucl. Instrum. Methods Phys. Res. B*, **266** (2008) 2683.
- [31] MOTTA A. T., *J. Nucl. Mater.*, **244** (1997) 227.